Eur. Phys. J. C (2021) 81:601
https://doi.org/10.1140/epjc/s10052-021-09305-3

THE EUROPEAN PHYSICAL JOURNAL C

Regular Article - Experimental Physics

Observation of new excited B_s^0 states

LHCb Collaboration[⋆]

CERN, 1211 Geneva 23, Switzerland

Received: 2 November 2020 / Accepted: 2 June 2021

Abstract A structure is observed in the $B^{\pm}K^{\mp}$ mass spectrum in a sample of proton–proton collisions at centre-of-mass energies of 7, 8, and 13 TeV, collected with the LHCb detector and corresponding to a total integrated luminosity of $9\,\text{fb}^{-1}$. The structure is interpreted as the result of overlapping excited B_s^0 states. With high significance, a two-peak hypothesis provides a better description of the data than a single resonance. Under this hypothesis the masses and widths of the two states, assuming they decay directly to $B^{\pm}K^{\mp}$, are determined to be

$$m_1 = 6063.5 \pm 1.2\,(\text{stat}) \pm 0.8\,(\text{syst})\,\text{MeV},$$
$$\Gamma_1 = 26 \pm 4\,(\text{stat}) \pm 4\,(\text{syst})\,\text{MeV},$$
$$m_2 = 6114 \pm 3\,(\text{stat}) \pm 5\,(\text{syst})\,\text{MeV},$$
$$\Gamma_2 = 66 \pm 18\,(\text{stat}) \pm 21\,(\text{syst})\,\text{MeV}.$$

Alternative values assuming a decay through $B^{*\pm}K^{\mp}$, with a missing photon from the $B^{*\pm} \to B^{\pm}\gamma$ decay, which are shifted by approximately 45 MeV, are also determined. The possibility of a single state decaying in both channels is also considered. The ratio of the total production cross-section times branching fraction of the new states relative to the previously observed B_{s2}^{*0} state is determined to be $0.87 \pm 0.15\,(\text{stat}) \pm 0.19\,(\text{syst})$.

1 Introduction

The constituent quark model [1–3] has been very successful describing the quark composition and allowed quantum numbers of observed hadron states. Potential models exploiting heavy-quark symmetry [4–6] are used to calculate properties of mesons containing one heavy and one light quark, including those with $\bar{b}s$ quark content, termed collectively the B_s^{**0} mesons. Yet it is still difficult to predict precise masses and widths of such states. Experimental measurements are therefore essential. This paper presents an observation of an excess in the B^+K^- invariant-mass spectrum,[1] which we interpret as originating from B_s^{**0} mesons. Two states, B_{s1}^0 and B_{s2}^{*0}, with masses higher than the ground state B_s^0 and B_s^{*0} mesons have been previously observed [7–11]. Based on their masses and narrow widths, they are interpreted as two of the predicted states with orbital angular momentum $L = 1$. We report the ratio of the production cross-section times branching fraction for the newly observed states relative to that of the B_{s2}^{*0} meson.

Predictions using a variety of methods have been made for masses and widths of states belonging to orbital or radial excitations of $\bar{b}s$ states [12–18]. The spectroscopic notation, $n^{2S+1}L_J$, is commonly used to refer to these states, where n gives the radial quantum number, S the sum of the quark spins, L the orbital angular momentum of the quarks, and J the total angular momentum. The masses of the first radially excited states, 2^1S_0 and 2^3S_1, are predicted in the range between 5920 MeV and 6020 MeV.[2] Different calculations give significantly different predicted widths for these states. In some cases they are close to 100 MeV or more [12–14] and in others can be less than 50 MeV [15–17]. Broad states are difficult to identify experimentally, however, because of large non-resonant continuum contributions. The first D-wave states ($L = 2$) are predicted to have masses ranging roughly from 6050 to 6200 MeV. The 1^3D_3 state is almost always predicted to be relatively narrow, with a width less than 50 MeV. The $J = 2$ states 1^1D_2 and 1^3D_2 can mix, and depending on the mixing angle they may produce one of the states as narrow as 20 MeV. With multiple states potentially decaying to both the B^+K^- final state directly and through a B^{*+} intermediate state, with a missing photon from the $B^{*+} \to B^+\gamma$ decay, the observation of overlapping peaks in this mass region seems likely.

⋆ e-mail: msrudolp@syr.edu

[1] The inclusion of charge-conjugate processes is implied throughout.

[2] Natural units with $c = 1$ are used throughout.

Published online: 12 July 2021

2 Detector and selection

The LHCb detector [19,20] is a single-arm forward spectrometer covering the pseudorapidity range $2 < \eta < 5$, designed for the study of particles containing b or c quarks. The detector includes a high-precision tracking system consisting of a silicon-strip vertex detector surrounding the pp interaction region, a large-area silicon-strip detector located upstream of a dipole magnet with a bending power of about 4 Tm, and three stations of silicon-strip detectors and straw drift tubes placed downstream of the magnet. The tracking system provides a measurement of momentum, p, of charged particles with a relative uncertainty that varies from 0.5% at low momentum to 1.0% at 200 GeV. The minimum distance of a track to a primary pp interaction vertex (PV), the impact parameter (IP), is measured with a resolution of $(15 + 29/p_{\mathrm{T}})\,\mu$m, where p_{T} is the component of the momentum transverse to the beam, in GeV. Different types of charged hadrons are distinguished using information from two ring-imaging Cherenkov detectors. Photons, electrons and hadrons are identified by a calorimeter system consisting of scintillating-pad and preshower detectors, an electromagnetic calorimeter and a hadronic calorimeter. Muons are identified by a system composed of alternating layers of iron and multiwire proportional chambers. The online event selection is performed by a trigger, which consists of a hardware stage, based on information from the calorimeter and muon systems, followed by a software stage, which applies a full event reconstruction. At the hardware trigger stage, events are required to have a muon with high p_{T} or a hadron with high transverse energy in the calorimeter. The software trigger requires a two-, three- or four-track vertex with a significant displacement from any PV. At least one charged particle must have a $p_{\mathrm{T}} > 1.6$ GeV and be inconsistent with originating from a PV. Consistency with a PV is defined based on the χ^2 difference between vertex fits including and excluding the particle under consideration.

We use data samples collected from 2011 to 2018, at centre-of-mass energies of 7, 8, and 13 TeV, corresponding to an integrated luminosity of 9 fb^{-1}. We simulate both B_{s2}^{*0} decays and decays of a B_s^{**0} meson with a mass of 300 MeV above the B^+K^- mass threshold. In the simulation, pp collisions are generated using Pythia [21,22] with a specific LHCb configuration [23]. Decays of hadronic particles are described by EvtGen [24]. The interaction of the generated particles with the detector and its response are implemented using the Geant4 toolkit [25,26] as described in Ref. [27].

The selection of the B^+K^- candidates is performed in two steps. First, we select B^+ candidates using the decays $B^+ \to J/\psi K^+$ and $B^+ \to \overline{D}{}^0\pi^+$, with $J/\psi \to \mu^+\mu^-$ and $\overline{D}{}^0 \to K^+\pi^-$. Each final-state particle is formed from a high-quality track that is inconsistent with being produced at any PV in the event. Each kaon, pion and muon is also required to have particle identification information consistent with its hypothesis. We do not require the candidate to have fired the trigger in the event. The selection of B^+ candidates has high purity, with a background contribution in the B^+ mass region of less than 10%.

Subsequently, we form the B_s^{**0} candidates by combining the B^+ candidate with a K^- candidate consistent with being produced at the PV, referred to as the prompt kaon. In the same way we also select a separate sample of same-sign B^+K^+ candidates further used for constraining combinatorial background. Strong particle-identification requirements are applied to the prompt kaons to reduce the large pion background. As observed for the known B_{s2}^{*0} resonance, the strongest discriminant between resonant signals and combinatorial background is the kaon transverse momentum. We therefore study the B_s^{**0} candidates in bins of the prompt kaon p_{T}: $0.5 < p_{\mathrm{T}} < 1$ GeV, $1 < p_{\mathrm{T}} < 2$ GeV, and $p_{\mathrm{T}} > 2$ GeV. The B_s^{**0} candidate mass, $m_{B^+K^-}$, is reconstructed constraining the masses J/ψ or $\overline{D}{}^0$ meson and the B^+ meson to their known values [28] and requiring the B^+ candidate to have been produced at the PV. We search for new states in a spectrum of the mass difference, $\Delta m = m_{B^+K^-} - m_{B^+} - m_{K^-}$, where the latter two masses refer to the known B^+ and K^- masses [28]. The Δm spectrum, measured in the three kaon p_{T} regions, is shown in Fig. 1. A clear deviation from a smooth continuum shape is observed at approximately 300 MeV above the mass threshold, and is consistently present in both B^+ selections.

3 Fit description and results

We determine the significance of the excess using an unbinned maximum-likelihood fit to the B^+K^- mass difference spectrum in the region from 150 MeV to 800 MeV above the kinematic threshold. The fit is performed simultaneously in three bins of the prompt kaon p_{T}.

We form the background distribution from two components. The first is the combinatorial background, whose shape and yield are fixed based on a fit to the same-sign B^+K^+ mass difference distribution using a threshold function of the form $f(\Delta m) = \Delta m^a \exp(-b\Delta m)$, with a and b as free parameters. The additional continuum background component that is not present in the same-sign sample, and which arises from associated production (AP) of the non-resonant B^+K^- pairs, is free to vary in the fit; our model for this component is a second-degree polynomial. Given the similarity of the combinatorial and AP background shapes, statistical uncertainties in the former are expressed through the latter fit component.

The B_s^{**0} signal is described by one or two relativistic Breit–Wigner distributions, convolved with resolution functions determined using simulation. For new states, the decay

products' angular momentum (ℓ) is unknown, making it difficult to assign an appropriate Blatt–Weisskopf barrier factor [29]. The B_s^{**0} state most consistently predicted to be narrow decays with a $B^{(*)+}K^-$ angular momentum of $\ell = 3$, so we use this as default, but consider other angular momenta in alternative fits. The barrier radius parameter is fixed to 4 GeV^{-1} [30,31]. When fitting with two peaks, no interference between the two new states is considered. Interference is possible if the two states are both $J = 2$ mixed D-wave states, but in that case one of the states should be much wider, so this scenario is unlikely to produce two narrow peaks.

We use two resolution models: one where the decay goes directly to a B^+K^- final state and the other where it proceeds through an intermediate B^{*+} meson which decays to $B^+\gamma$. We model the resolution in the direct B^+K^- decay as the sum of a Gaussian distribution and a Crystal Ball function [32] with a shared mean, and in the $B^{*+}K^-$ channel as the sum of two Gaussian distributions with different means to account for the smearing and shift in the peak position by approximately 45 MeV due to the unreconstructed photon. The detector resolution is small compared to the width of the prospective states; the effect of the missing photon is significant. The peak positions and widths are shared in each bin of the kaon p_{T}, but the yield is allowed to vary independently. The fit results using the polynomial AP shape are shown in Fig. 1. A total signal yield of $18\,900 \pm 2200$ is observed in the two peaks across all the p_{T} bins when fit with the default model and B^+K^- resolution.

We determine the local statistical significance of the observation using the asymptotic formula for the profile likelihood ratio test statistic [33]. We compare first the one-peak hypothesis to the null hypothesis, and then the two-peak to the one-peak hypothesis. The null fit model corresponds to only a polynomial description of the AP in addition to the shape of the same-sign data. The minimum of the test statistics across each fit with different AP descriptions (discussed later) gives local significances of more than 20σ for the one-peak fit with respect to the null hypothesis and 7.7σ for the two-peak description with respect to the one-peak hypothesis. As the significance is large, we have not made an exact quantification of the penalty due to the look-elsewhere effect.

Assuming the two-peak hypothesis, the masses and widths of the two states and the fraction of the yield in the lower mass state, f_1, are determined to be

$$
\begin{aligned}
m_1 &= 6063.5 \pm 1.2\,(\mathrm{stat}) \pm 0.8\,(\mathrm{syst})\,\mathrm{MeV},\\
\Gamma_1 &= 26 \pm 4\,(\mathrm{stat}) \pm 4\,(\mathrm{syst})\,\mathrm{MeV},\\
m_2 &= 6114 \pm 3\,(\mathrm{stat}) \pm 5\,(\mathrm{syst})\,\mathrm{MeV},\\
\Gamma_2 &= 66 \pm 18\,(\mathrm{stat}) \pm 21\,(\mathrm{syst})\,\mathrm{MeV},\\
f_1 &= 0.47 \pm 0.11\,(\mathrm{stat}) \pm 0.15\,(\mathrm{syst}),
\end{aligned}
$$

if the decay is directly to the B^+K^- final state. If it instead proceeds through $B^{*+}K^-$, they are

$$
\begin{aligned}
m_1 &= 6108.8 \pm 1.1\,(\mathrm{stat}) \pm 0.7\,(\mathrm{syst})\,\mathrm{MeV},\\
\Gamma_1 &= 22 \pm 5\,(\mathrm{stat}) \pm 4\,(\mathrm{syst})\,\mathrm{MeV},\\
m_2 &= 6158 \pm 4\,(\mathrm{stat}) \pm 5\,(\mathrm{syst})\,\mathrm{MeV},\\
\Gamma_2 &= 72 \pm 18\,(\mathrm{stat}) \pm 25\,(\mathrm{syst})\,\mathrm{MeV},\\
f_1 &= 0.42 \pm 0.11\,(\mathrm{stat}) \pm 0.16\,(\mathrm{syst}).
\end{aligned}
$$

The dominant contribution to the systematic uncertainty arises from the considered variations in the fit functions, and is obtained by repeating the fits with different conditions and calculating the differences with the default fit. We refit the data sample using alternative functional forms for the AP background: an exponential and a separate threshold function. Each AP description produces consistent results for the significance, with variation in the peak parameters. The dependence on the signal model is estimated by alternatively using relativistic Breit-Wigner models with different angular-momentum hypotheses of $\ell = 2$ or $\ell = 1$ and taking the largest absolute difference. We also vary the p_{T} binning and mass range for the fit, and we include the effect on one peak's parameters of changing the other peak from the B^+K^- model to the $B^{*+}K^-$ model or vice versa. A breakdown of the systematic uncertainties is given in Table 1.

Since the mass difference between the two peaks is found to be close to the B^{*+}–B^+ mass difference of approximately 45 MeV, we consider also the possibility that the structure is produced by a single resonance that decays in both the B^+K^- and $B^{*+}K^-$ channels. In an alternative fit, both resolution models are simultaneously combined with a resonance lineshape described by a single mass and width. This hypothesis is disfavored by more than 2σ with respect to the two-state hypothesis and cannot be completely ruled out. Qualitatively, this model does not describe the data as well because the observed width is much different in the two peaks, with the lower peak being narrower.

4 Production ratio

In addition to the masses and widths of the new mesons, we also determine the production ratio relative to the B_{s2}^{*0} meson. The B^+K^- candidates in both mass ranges are selected as previously described, but we use only candidates selected from the $B^+ \to J/\psi K^+$ decay and require the candidate to have triggered the event. We define the production ratio as the product of the cross-sections times branching fractions of the new states divided by the corresponding product for B_{s2}^{*0},

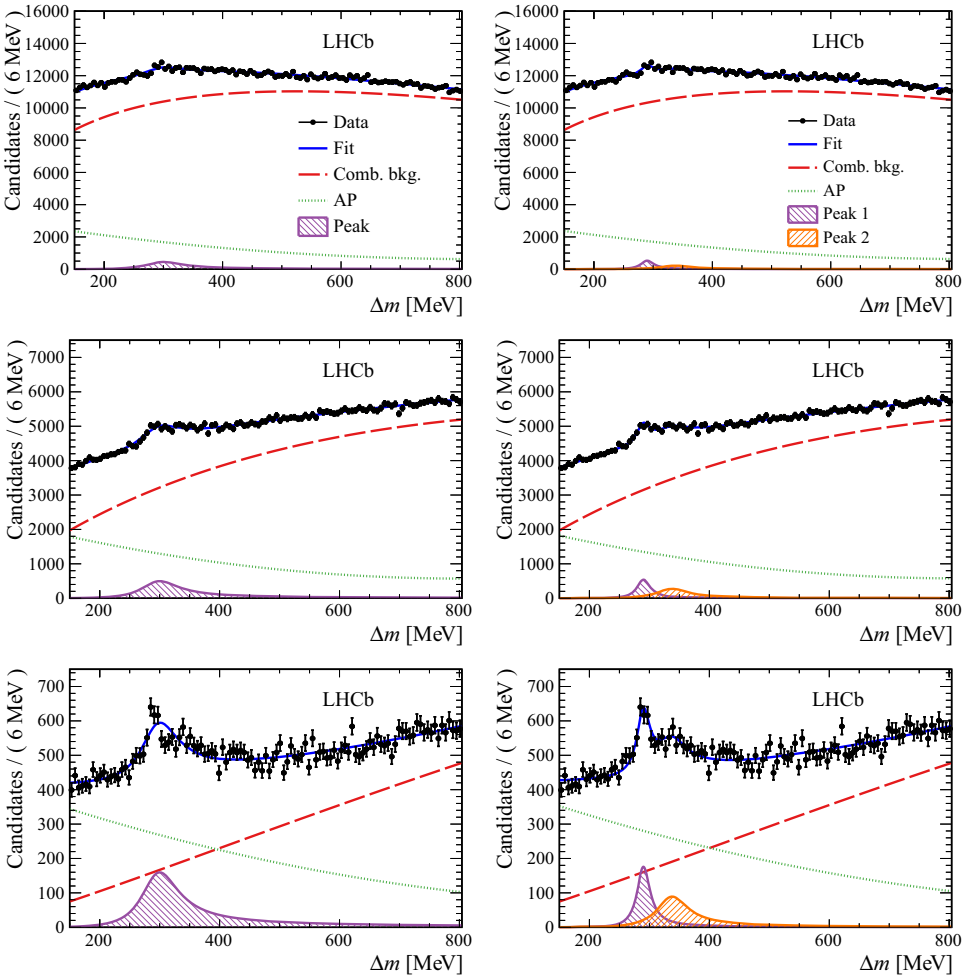

Fig. 1 The B^+K^- mass difference distributions in data, overlaid with the fit models: (left column) one-peak hypothesis and (right column) two-peak hypothesis. In each column, the rows are from top to bottom for candidates with the prompt kaon p_T: $0.5 < p_T < 1$ GeV, $1 < p_T < 2$ GeV, and $p_T > 2$ GeV. The legend in the top row applies for each column. The associated production (AP) background is described by a second-degree polynomial in each fit. The combinatorial background shape is fixed from a fit to the B^+K^+ mass difference distributions

Table 1 Sources of systematic uncertainty on the peak parameters assuming a two-peak structure decaying either directly to B^+K^- or through $B^{*+}K^-$. The parameter differences with respect to the nominal fit result are given in MeV

Decay hypothesis	Source	m_1	Γ_1	m_2	Γ_2	f_1
B^+K^-	Background model	0.4	1.2	0.7	10.6	0.07
	Signal model	0.5	3.9	4.3	11.5	0.11
	Mass and p_T range	0.4	1.3	1.6	13.6	0.07
	Total	0.8	4.2	4.6	20.7	0.15
$B^{*+}K^-$	Background model	0.4	1.7	0.7	13.1	0.08
	Signal model	0.2	3.3	4.2	9.0	0.08
	Mass and p_T range	0.5	2.1	1.3	19.5	0.10
	Total	0.7	4.3	4.5	25.1	0.16

$$R = \frac{\sum \sigma(B_s^{**0}) \times \mathcal{B}(B_s^{**0} \to B^{(*)+}K^-)}{\sigma(B_{s2}^{*0}) \times \mathcal{B}(B_{s2}^{*0} \to B^+K^-)}. \quad (1)$$

We sum the measured yield for both observed states, and consider the yield difference of the B^+K^- and $B^{*+}K^-$ models as a systematic uncertainty. The ratio is taken with respect to the yield for only the B^+K^- decay of the B_{s2}^{*0} meson. The production cross-section is restricted to the fiducial region of B_s^{**0} transverse momentum and rapidity, $0 < p_T < 20$ GeV and $2.1 < y < 4.2$.

The relative efficiency for a state at the observed mass with respect to the B_{s2}^{*0} meson is determined using simulation, and used to correct the observed yields. The largest systematic uncertainty on the relative efficiency comes from

Table 2 Summary of the systematic uncertainties on the production ratio. The effect of the unknown p_T distribution is separated from other uncertainties affecting the relative efficiency

Source	Absolute uncertainty
Signal fit variations	0.10
Background fit variations	0.10
Mass and p_T range variations	0.13
B_s^{**0} p_T distribution	0.02
Other efficiency uncertainties	0.02
Total	0.19

the unknown transverse momentum spectra of the new states. Additional efficiency uncertainties, for example from the description of particle identification in simulation, give smaller contributions. The B_{s2}^{*0} yield is determined from a separate unbinned maximum-likelihood fit in the range $50 < \Delta m < 85$ MeV, using the same prompt kaon p_T binning as in the main fit. The systematic uncertainties from signal and background fit-model variations are handled as in the fit used for the observation. The fit is additionally separated into different data-taking periods since the efficiency and production ratio may depend on the collision energy and detector conditions. The results, however, are statistically compatible between the different periods. We therefore quote the combined production ratio

$$R = 0.87 \pm 0.15\,(\text{stat}) \pm 0.19\,(\text{syst}).$$

A breakdown of the systematic uncertainties is given in Table 2.

5 Conclusions

An excess is observed in the B^+K^- mass spectrum at a mass approximately 300 MeV above the B^+K^- threshold, which we interpret as resulting from the decays of multiple excited B_s^{**0} mesons. The structure is not well described by a single resonance; the significance for a two-peak structure relative to a one-peak hypothesis is greater than 7σ. A single resonance which can decay through both the B^+K^- and $B^{*+}K^-$ channels is disfavoured but cannot be excluded. Future investigation with a larger data sample and with the $B^{*+}K^-$ final state fully reconstructed could potentially better determine the exact structure in this mass range. Under the two-peak hypothesis, we have measured the masses and widths of the two states. Based on predictions for the masses of excited B_s^{*0} states, the new observation is likely to result from $L = 2$ orbitally excited mesons. We have additionally determined the production cross-section times branching fraction of the new excess relative to the previously observed $L = 1$ B_{s2}^{*0}, which shows that it is produced at a comparable rate.

Acknowledgements We express our gratitude to our colleagues in the CERN accelerator departments for the excellent performance of the LHC. We thank the technical and administrative staff at the LHCb institutes. We acknowledge support from CERN and from the national agencies: CAPES, CNPq, FAPERJ and FINEP (Brazil); MOST and NSFC (China); CNRS/IN2P3 (France); BMBF, DFG and MPG (Germany); INFN (Italy); NWO (Netherlands); MNiSW and NCN (Poland); MEN/IFA (Romania); MSHE (Russia); MICINN (Spain); SNSF and SER (Switzerland); NASU (Ukraine); STFC (United Kingdom); DOE NP and NSF (USA). We acknowledge the computing resources that are provided by CERN, IN2P3 (France), KIT and DESY (Germany), INFN (Italy), SURF (Netherlands), PIC (Spain), GridPP (United Kingdom), RRCKI and Yandex LLC (Russia), CSCS (Switzerland), IFIN-HH (Romania), CBPF (Brazil), PL-GRID (Poland) and OSC (USA). We are indebted to the communities behind the multiple open-source software packages on which we depend. Individual groups or members have received support from AvH Foundation (Germany); EPLANET, Marie Skłodowska-Curie Actions and ERC (European Union); A*MIDEX, ANR, Labex P2IO and OCEVU, and Région Auvergne-Rhône-Alpes (France); Key Research Program of Frontier Sciences of CAS, CAS PIFI, Thousand Talents Program, and Sci. & Tech. Program of Guangzhou (China); RFBR, RSF and Yandex LLC (Russia); GVA, XuntaGal and GENCAT (Spain); the Royal Society and the Leverhulme Trust (United Kingdom).

Data Availability Statement This manuscript has no associated data or the data will not be deposited. [Authors' comment: All LHCb scientific output is published in journals, with preliminary results made available in Conference Reports. All are Open Access, without restriction on use beyond the standard conditions agreed by CERN. Data associated to the plots in this publication as well as in supplementary materials are made available on the CERN document server at http://cdsweb.cern.ch/record/2743367. This information is taken from the LHCb External Data Access Policy which can be downloaded at http://opendata.cern.ch/record/410.]

Funded by SCOAP[3].

References

1. M. Gell-Mann, A schematic model of baryons and mesons. Phys. Lett. **8**, 214 (1964). https://doi.org/10.1016/S0031-9163(64)92001-3
2. G. Zweig, An SU_3 Model for Strong Interaction Symmetry and Its Breaking; Version 1 CERN-TH-401 CERN, Geneva (1964)
3. G. Zweig, An SU_3 model for strong interaction symmetry and its breaking. Version 2, CERN-TH-412 (1964)

4. S. Godfrey, N. Isgur, Mesons in a relativized quark model with chromodynamics. Phys. Rev. D **32**, 189 (1985). https://doi.org/10.1103/PhysRevD.32.189
5. M. Neubert, Heavy-quark symmetry. Phys. Rep. **245**, 259 (1994). https://doi.org/10.1016/0370-1573(94)90091-4
6. A.V. Manohar, M.B. Wise, Heavy Quark Phys. **10** (2000)
7. CDF collaboration, T. Aaltonen et al., Observation of orbitally excited B_s mesons. Phys. Rev. Lett. **100**, 082001, (2008). https://doi.org/10.1103/PhysRevLett.100.082001. arXiv:0710.4199
8. D0 collaboration, V.M. Abazov et al., Observation and properties of the orbitally excited B^*_{s2} meson. Phys. Rev. Lett. **100**, 082002, (2008). https://doi.org/10.1103/PhysRevLett.100.082002. arXiv:0711.0319
9. LHCb collaboration, R. Aaij et al., First observation of the decay $B^*_{s2}(5840)^0 \to B^{*+}K^-$ and studies of excited B^0_s mesons. Phys. Rev. Lett. **110**, 151803 (2013). https://doi.org/10.1103/PhysRevLett.110.151803. arXiv:1211.5994
10. CDF collaboration, T. Aaltonen et al., Study of orbitally excited B mesons and evidence for a new $B\pi$ resonance. Phys. Rev. D **90**, 012013 (2014). https://doi.org/10.1103/PhysRevD.90.012013. arXiv:1309.5961
11. CMS Collaboration, Studies of $B^*_{s2}(5840)^0$ and $B_{s1}(5830)^0$ mesons including the observation of the $B^*_{s2}(5840)^0 \to B^0 K^0_S$ decay in proton-proton collisions at $\sqrt{s} = 8$ TeV. Eur. Phys. J. C **78**, 939 (2018). https://doi.org/10.1140/epjc/s10052-018-6390-z. arXiv:1809.03578
12. S. Godfrey, K. Moats, E.S. Swanson, B and B_s meson spectroscopy. Phys. Rev. D **94**, 054025 (2016). https://doi.org/10.1103/PhysRevD.94.054025 arXiv:1607.02169
13. J. Ferretti, E. Santopinto, Open-flavor strong decays of open-charm and open-bottom mesons in the $^3P_0$ model. Phys. Rev. D **97**, 114020 (2018). https://doi.org/10.1103/PhysRevD.97.114020 arXiv:1506.04415
14. Q.-F. Lü et al., Excited bottom and bottom-strange mesons in the quark model. Phys. Rev. D **94**, 074012 (2016). https://doi.org/10.1103/PhysRevD.94.074012 arXiv:1607.02812
15. L.-Y. Xiao, X.-H. Zhong, Strong decays of higher excited heavy-light mesons in a chiral quark model. Phys. Rev. D **90**, 074029 (2014). https://doi.org/10.1103/PhysRevD.90.074029 arXiv:1407.7408
16. Y. Sun et al., Higher bottom and bottom-strange mesons. Phys. Rev. D **89**, 054026 (2014). https://doi.org/10.1103/PhysRevD.89.054026 arXiv:1401.1595
17. I. Asghar et al., Decays and spectrum of bottom and bottom strange mesons. Eur. Phys. J. A **54**, 127 (2018). https://doi.org/10.1140/epja/i2018-12558-6 arXiv:1804.08802
18. J.-B. Liu, M.-Z. Yang, Spectrum of higher excitations of B and D mesons in the relativistic potential model. Phys. Rev. D **91**, 094004 (2015). https://doi.org/10.1103/PhysRevD.91.094004 arXiv:1501.04266
19. LHCb collaboration, A.A. Alves Jr. et al., The LHCb detector at the LHC. JINST **3**, S08005 (2008). https://doi.org/10.1088/1748-0221/3/08/S08005
20. LHCb collaboration, R. Aaij et al., LHCb detector performance. Int. J. Mod. Phys. A **30**, 1530022 (2015). https://doi.org/10.1142/S0217751X15300227. arXiv:1412.6352
21. T. Sjöstrand, S. Mrenna, P. Skands, PYTHIA 6.4 physics and manual. JHEP **05**, 026 (2006). https://doi.org/10.1088/1126-6708/2006/05/026 arXiv:hep-ph/0603175
22. T. Sjöstrand, S. Mrenna, P. Skands, A brief introduction to PYTHIA 8.1. Comput. Phys. Commun. **178**, 852 (2008). https://doi.org/10.1016/j.cpc.2008.01.036 arXiv:0710.3820
23. I. Belyaev et al., Handling of the generation of primary events in Gauss, the LHCb simulation framework. J. Phys. Conf. Ser. **331**, 032047 (2011). https://doi.org/10.1088/1742-6596/331/3/032047
24. D.J. Lange, The EvtGen particle decay simulation package. Nucl. Instrum. Methods **A462**, 152 (2001). https://doi.org/10.1016/S0168-9002(01)00089-4
25. Geant4 collaboration, J. Allison et al., Geant4 developments and applications. IEEE Trans. Nucl. Sci. **53**, 270 (2006). https://doi.org/10.1109/TNS.2006.869826
26. Geant4 collaboration, S. Agostinelli et al., Geant4: a simulation toolkit. Nucl. Instrum. Methods A **506**, 250 (2003). https://doi.org/10.1016/S0168-9002(03)01368-8
27. M. Clemencic et al., The LHCb simulation application, Gauss: design, evolution and experience. J. Phys. Conf. Ser. **331**, 032023 (2011). https://doi.org/10.1088/1742-6596/331/3/032023
28. Particle Data Group, P.A. Zyla et al., Review of particle physics. Prog. Theor. Exp. Phys. **2020**, 083C01 (2020). https://doi.org/10.1093/ptep/ptaa104
29. J.M. Blatt, V.F. Weisskopf, *Theoretical Nuclear Physics* (Springer, New York, 1952). https://doi.org/10.1007/978-1-4612-9959-2
30. LHCb collaboration, R. Aaij et al., Dalitz plot analysis of $B^0_s \to \overline{D}^0 K^- \pi^+$ decays. Phys. Rev. D **90**, 072003 (2014). https://doi.org/10.1103/PhysRevD.90.072003. arXiv:1407.7712
31. LHCb collaboration, R. Aaij et al., Precise measurements of the properties of the $B_1(5721)^{0,+}$ and $B^*_2(5747)^{0,+}$ states and observation of structure at higher invariant mass in the $B^+\pi^-$ and $B^0\pi^+$ spectra. JHEP **04**, 024 (2015). https://doi.org/10.1007/JHEP04(2015)024. arXiv:1502.02638
32. T. Skwarnicki, A study of the radiative cascade transitions between the Upsilon-prime and Upsilon resonances, Ph.D. thesis, Institute of Nuclear Physics, Krakow, 1986, DESY-F31-86-02
33. S.S. Wilks, The large-sample distribution of the likelihood ratio for testing composite hypotheses. Ann. Math. Stat. **9**, 60 (1938). https://doi.org/10.1214/aoms/1177732360

LHCb Collaboration[⋆]

R. Aaij[31], C. Abellán Beteta[49], T. Ackernley[59], B. Adeva[45], M. Adinolfi[53], H. Afsharnia[9], C. A. Aidala[84], S. Aiola[25], Z. Ajaltouni[9], S. Akar[64], J. Albrecht[14], F. Alessio[47], M. Alexander[58], A. Alfonso Albero[44], Z. Aliouche[61], G. Alkhazov[37], P. Alvarez Cartelle[47], S. Amato[2], Y. Amhis[11], L. An[21], L. Anderlini[21], A. Andreianov[37], M. Andreotti[20], F. Archilli[16], A. Artamonov[43], M. Artuso[67], K. Arzymatov[41], E. Aslanides[10], M. Atzeni[49], B. Audurier[11], S. Bachmann[16], M. Bachmayer[48], J. J. Back[55], S. Baker[60], P. Baladron Rodriguez[45], V. Balagura[11], W. Baldini[20], J. Baptista Leite[1], R. J. Barlow[61], S. Barsuk[11], W. Barter[60], M. Bartolini[23,i], F. Baryshnikov[80], J. M. Basels[13], G. Bassi[28], B. Batsukh[67], A. Battig[14], A. Bay[48], M. Becker[14], F. Bedeschi[28], I. Bediaga[1], A. Beiter[67], V. Belavin[41], S. Belin[26], V. Bellee[48], K. Belous[43], I. Belov[39], I. Belyaev[38], G. Bencivenni[22], E. Ben-Haim[12], A. Berezhnoy[39], R. Bernet[49], D. Berninghoff[16], H. C. Bernstein[67], C. Bertella[47], E. Bertholet[12], A. Bertolin[27], C. Betancourt[49], F. Betti[19,e], M. O. Bettler[54], Ia. Bezshyiko[49], S. Bhasin[53], J. Bhom[33], L. Bian[72], M. S. Bieker[14], S. Bifani[52], P. Billoir[12], M. Birch[60], F. C. R. Bishop[54], A. Bizzeti[21,s], M. Bjørn[62], M. P. Blago[47], T. Blake[55], F. Blanc[48], S. Blusk[67], D. Bobulska[58], J. A. Boelhauve[14], O. Boente Garcia[45], T. Boettcher[63], A. Boldyrev[81], A. Bondar[42,v], N. Bondar[37], S. Borghi[61], M. Borisyak[41], M. Borsato[16], J. T. Borsuk[33], S. A. Bouchiba[48], T. J. V. Bowcock[59], A. Boyer[47], C. Bozzi[20], M. J. Bradley[60], S. Braun[65], A. Brea Rodriguez[45], M. Brodski[47], J. Brodzicka[33], A. Brossa Gonzalo[55], D. Brundu[26], A. Buonaura[49], C. Burr[47], A. Bursche[26], A. Butkevich[40], J. S. Butter[31], J. Buytaert[47], W. Byczynski[47], S. Cadeddu[26], H. Cai[72], R. Calabrese[20,g], L. Calefice[14], L. Calero Diaz[22], S. Cali[22], R. Calladine[52], M. Calvi[24,j], M. Calvo Gomez[83], P. Camargo Magalhaes[53], A. Camboni[44], P. Campana[22], D. H. Campora Perez[47], A. F. Campoverde Quezada[5], S. Capelli[24,j], L. Capriotti[19,e], A. Carbone[19,e], G. Carboni[29], R. Cardinale[23,i], A. Cardini[26], I. Carli[6], P. Carniti[24,j], K. Carvalho Akiba[31], A. Casais Vidal[45], G. Casse[59], M. Cattaneo[47], G. Cavallero[47], S. Celani[48], J. Cerasoli[10], A. J. Chadwick[59], M. G. Chapman[53], M. Charles[12], Ph. Charpentier[47], G. Chatzikonstantinidis[52], C. A. Chavez Barajas[59], M. Chefdeville[8], C. Chen[3], S. Chen[26], A. Chernov[33], S.-G. Chitic[47], V. Chobanova[45], S. Cholak[48], M. Chrzaszcz[33], A. Chubykin[37], V. Chulikov[37], P. Ciambrone[22], M. F. Cicala[55], X. Cid Vidal[45], G. Ciezarek[47], P. E. L. Clarke[57], M. Clemencic[47], H. V. Cliff[54], J. Closier[47], J. L. Cobbledick[61], V. Coco[47], J. A. B. Coelho[11], J. Cogan[10], E. Cogneras[9], L. Cojocariu[36], P. Collins[47], T. Colombo[47], L. Congedo[18], A. Contu[26], N. Cooke[52], G. Coombs[58], G. Corti[47], C. M. Costa Sobral[55], B. Couturier[47], D. C. Craik[63], J. Crkovská[66], M. Cruz Torres[1], R. Currie[57], C. L. Da Silva[66], E. Dall'Occo[14], J. Dalseno[45], C. D'Ambrosio[47], A. Danilina[38], P. d'Argent[47], A. Davis[61], O. De Aguiar Francisco[61], K. De Bruyn[77], S. De Capua[61], M. De Cian[48], J. M. De Miranda[1], L. De Paula[2], M. De Serio[18,d], D. De Simone[49], P. De Simone[22], J. A. de Vries[78], C. T. Dean[66], W. Dean[84], D. Decamp[8], L. Del Buono[12], B. Delaney[54], H.-P. Dembinski[14], A. Dendek[34], V. Denysenko[49], D. Derkach[81], O. Deschamps[9], F. Desse[11], F. Dettori[26,f], B. Dey[72], P. Di Nezza[22], S. Didenko[80], L. Dieste Maronas[45], H. Dijkstra[47], V. Dobishuk[51], A. M. Donohoe[17], F. Dordei[26], A. C. dos Reis[1], L. Douglas[58], A. Dovbnya[50], A. G. Downes[8], K. Dreimanis[59], M. W. Dudek[33], L. Dufour[47], V. Duk[76], P. Durante[47], J. M. Durham[66], D. Dutta[61], M. Dziewiecki[16], A. Dziurda[33], A. Dzyuba[37], S. Easo[56], U. Egede[68], V. Egorychev[38], S. Eidelman[42,v], S. Eisenhardt[57], S. Ek-In[48], L. Eklund[58], S. Ely[67], A. Ene[36], E. Epple[66], S. Escher[13], J. Eschle[49], S. Esen[31], T. Evans[47], A. Falabella[19], J. Fan[3], Y. Fan[5], B. Fang[72], N. Farley[52], S. Farry[59], D. Fazzini[24,j], P. Fedin[38], M. Féo[47], P. Fernandez Declara[47], A. Fernandez Prieto[45], J. M. Fernandez-tenllado Arribas[44], F. Ferrari[19,e], L. Ferreira Lopes[48], F. Ferreira Rodrigues[2], S. Ferreres Sole[31], M. Ferrillo[49], M. Ferro-Luzzi[47], S. Filippov[40], R. A. Fini[18], M. Fiorini[20,g], M. Firlej[34], K. M. Fischer[62], C. Fitzpatrick[61], T. Fiutowski[34], F. Fleuret[11,b], M. Fontana[47], F. Fontanelli[23,i], R. Forty[47], V. Franco Lima[59], M. Franco Sevilla[65], M. Frank[47], E. Franzoso[20], G. Frau[16], C. Frei[47], D. A. Friday[58], J. Fu[25], Q. Fuehring[14], W. Funk[47], E. Gabriel[31], T. Gaintseva[41], A. Gallas Torreira[45], D. Galli[19,e], S. Gambetta[57], Y. Gan[3], M. Gandelman[2], P. Gandini[25], Y. Gao[4], M. Garau[26], L. M. Garcia Martin[55], P. Garcia Moreno[44], J. García Pardiñas[49], B. Garcia Plana[45], F. A. Garcia Rosales[11], L. Garrido[44], D. Gascon[44], C. Gaspar[47], R. E. Geertsema[31], D. Gerick[16], L. L. Gerken[14], E. Gersabeck[61], M. Gersabeck[61], T. Gershon[55], D. Gerstel[10], Ph. Ghez[8], V. Gibson[54], M. Giovannetti[22,k], A. Gioventù[45], P. Gironella Gironell[44], L. Giubega[36], C. Giugliano[20,g], K. Gizdov[57], E. L. Gkougkousis[47], V. V. Gligorov[12], C. Göbel[69], E. Golobardes[83], D. Golubkov[38], A. Golutvin[60,80], A. Gomes[1,a], S. Gomez Fernandez[44], F. Goncalves Abrantes[69], M. Goncerz[33], G. Gong[3], P. Gorbounov[38], I. V. Gorelov[39], C. Gotti[24,j], E. Govorkova[31], J. P. Grabowski[16], R. Graciani Diaz[44], T. Grammatico[12], L. A. Granado Cardoso[47], E. Graugés[44], E. Graverini[48], G. Graziani[21], A. Grecu[36], L. M. Greeven[31], P. Griffith[20], L. Grillo[61], S. Gromov[80], L. Gruber[47], B. R. Gruberg Cazon[62], C. Gu[3], M. Guarise[20], P. A. Günther[16], E. Gushchin[40], A. Guth[13], Y. Guz[43,47], T. Gys[47], T. Hadavizadeh[68], G. Haefeli[48], C. Haen[47], J. Haimberger[47], S. C. Haines[54], T. Halewood-leagas[59], P. M. Hamilton[65], Q. Han[7], X. Han[16], T. H. Hancock[62], S. Hansmann-Menzemer[16], N. Harnew[62], T. Harrison[59], C. Hasse[47], M. Hatch[47], J. He[5], M. Hecker[60], K. Heijhoff[31], K. Heinicke[14], A. M. Hennequin[47], K. Hennessy[59], L. Henry[25,46], J. Heuel[13], A. Hicheur[2], D. Hill[62], M. Hilton[61], S. E. Hollitt[14], P. H. Hopchev[48], J. Hu[16], J. Hu[71], W. Hu[7], W. Huang[5], X. Huang[72], W. Hulsbergen[31], R. J. Hunter[55],

M. Hushchyn[81], D. Hutchcroft[59], D. Hynds[31], P. Ibis[14], M. Idzik[34], D. Ilin[37], P. Ilten[52], A. Inglessi[37], A. Ishteev[80], K. Ivshin[37], R. Jacobsson[47], S. Jakobsen[47], E. Jans[31], B. K. Jashal[46], A. Jawahery[65], V. Jevtic[14], M. Jezabek[33], F. Jiang[3], M. John[62], D. Johnson[47], C. R. Jones[54], T. P. Jones[55], B. Jost[47], N. Jurik[47], S. Kandybei[50], Y. Kang[3], M. Karacson[47], J. M. Kariuki[53], N. Kazeev[81], M. Kecke[16], F. Keizer[47,54], M. Kenzie[55], T. Ketel[32], B. Khanji[47], A. Kharisova[82], S. Kholodenko[43], K. E. Kim[67], T. Kirn[13], V. S. Kirsebom[48], O. Kitouni[63], S. Klaver[31], K. Klimaszewski[35], S. Koliiev[51], A. Kondybayeva[80], A. Konoplyannikov[38], P. Kopciewicz[34], R. Kopecna[16], P. Koppenburg[31], M. Korolev[39], I. Kostiuk[31,51], O. Kot[51], S. Kotriakhova[30,37], P. Kravchenko[37], L. Kravchuk[40], R. D. Krawczyk[47], M. Kreps[55], F. Kress[60], S. Kretzschmar[13], P. Krokovny[42,v], W. Krupa[34], W. Krzemien[35], W. Kucewicz[33,l], M. Kucharczyk[33], V. Kudryavtsev[42,v], H. S. Kuindersma[31], G. J. Kunde[66], T. Kvaratskheliya[38], D. Lacarrere[47], G. Lafferty[61], A. Lai[26], A. Lampis[26], D. Lancierini[49], J. J. Lane[61], R. Lane[53], G. Lanfranchi[22], C. Langenbruch[13], J. Langer[14], O. Lantwin[49,80], T. Latham[55], F. Lazzari[28,t], R. Le Gac[10], S. H. Lee[84], R. Lefèvre[9], A. Leflat[39], S. Legotin[80], O. Leroy[10], T. Lesiak[33], B. Leverington[16], H. Li[71], L. Li[62], P. Li[16], X. Li[66], Y. Li[6], Y. Li[6], Z. Li[67], X. Liang[67], T. Lin[60], R. Lindner[47], V. Lisovskyi[14], R. Litvinov[26], G. Liu[71], H. Liu[5], S. Liu[6], X. Liu[3], A. Loi[26], J. Lomba Castro[45], I. Longstaff[58], J. H. Lopes[2], G. Loustau[49], G. H. Lovell[54], Y. Lu[6], D. Lucchesi[27,m], S. Luchuk[40], M. Lucio Martinez[31], V. Lukashenko[31], Y. Luo[3], A. Lupato[61], E. Luppi[20,g], O. Lupton[55], A. Lusiani[28,r], X. Lyu[5], L. Ma[6], S. Maccolini[19,e], F. Machefert[11], F. Maciuc[36], V. Macko[48], P. Mackowiak[14], S. Maddrell-Mander[53], O. Madejczyk[34], L. R. Madhan Mohan[53], O. Maev[37], A. Maevskiy[81], D. Maisuzenko[37], M. W. Majewski[34], S. Malde[62], B. Malecki[47], A. Malinin[79], T. Maltsev[42,v], H. Malygina[16], G. Manca[26,f], G. Mancinelli[10], R. Manera Escalero[44], D. Manuzzi[19,e], D. Marangotto[25,o], J. Maratas[9,u], J. F. Marchand[8], U. Marconi[19], S. Mariani[21,47,h], C. Marin Benito[11], M. Marinangeli[48], P. Marino[48], J. Marks[16], P. J. Marshall[59], G. Martellotti[30], L. Martinazzoli[47,j], M. Martinelli[24,j], D. Martinez Santos[45], F. Martinez Vidal[46], A. Massafferri[1], M. Materok[13], R. Matev[47], A. Mathad[49], Z. Mathe[47], V. Matiunin[38], C. Matteuzzi[24], K. R. Mattioli[84], A. Mauri[31], E. Maurice[11,b], J. Mauricio[44], M. Mazurek[35], M. McCann[60], L. Mcconnell[17], T. H. Mcgrath[61], A. McNab[61], R. McNulty[17], J. V. Mead[59], B. Meadows[64], C. Meaux[10], G. Meier[14], N. Meinert[75], D. Melnychuk[35], S. Meloni[24,j], M. Merk[31,78], A. Merli[25], L. Meyer Garcia[2], M. Mikhasenko[47], D. A. Milanes[73], E. Millard[55], M. Milovanovic[47], M.-N. Minard[8], L. Minzoni[20,g], S. E. Mitchell[57], B. Mitreska[61], D. S. Mitzel[47], A. Mödden[14], R. A. Mohammed[62], R. D. Moise[60], T. Mombächer[14], I. A. Monroy[73], S. Monteil[9], M. Morandin[27], G. Morello[22], M. J. Morello[28,r], J. Moron[34], A. B. Morris[74], A. G. Morris[55], R. Mountain[67], H. Mu[3], F. Muheim[57], M. Mukherjee[7], M. Mulder[47], D. Müller[47], K. Müller[49], C. H. Murphy[62], D. Murray[61], P. Muzzetto[26], P. Naik[53], T. Nakada[48], R. Nandakumar[56], T. Nanut[48], I. Nasteva[2], M. Needham[57], I. Neri[20,g], N. Neri[25,o], S. Neubert[74], N. Neufeld[47], R. Newcombe[60], T. D. Nguyen[48], C. Nguyen-Mau[48], E. M. Niel[11], S. Nieswand[13], N. Nikitin[39], N. S. Nolte[47], C. Nunez[84], A. Oblakowska-Mucha[34], V. Obraztsov[43], D. P. O'Hanlon[53], R. Oldeman[26,f], C. J. G. Onderwater[77], A. Ossowska[33], J. M. Otalora Goicochea[2], T. Ovsiannikova[38], P. Owen[49], A. Oyanguren[46], B. Pagare[55], P. R. Pais[47], T. Pajero[28,47,r], A. Palano[18], M. Palutan[22], Y. Pan[61], G. Panshin[82], A. Papanestis[56], M. Pappagallo[18,d], L. L. Pappalardo[20,g], C. Pappenheimer[64], W. Parker[65], C. Parkes[61], C. J. Parkinson[45], B. Passalacqua[20], G. Passaleva[21], A. Pastore[18], M. Patel[60], C. Patrignani[19,e], C. J. Pawley[78], A. Pearce[47], A. Pellegrino[31], M. Pepe Altarelli[47], S. Perazzini[19], D. Pereima[38], P. Perret[9], K. Petridis[53], A. Petrolini[23,i], A. Petrov[79], S. Petrucci[57], M. Petruzzo[25], A. Philippov[41], L. Pica[28], M. Piccini[76], B. Pietrzyk[8], G. Pietrzyk[48], M. Pili[62], D. Pinci[30], J. Pinzino[47], F. Pisani[47], A. Piucci[16], Resmi P.K[10], V. Placinta[36], S. Playfer[57], J. Plews[52], M. Plo Casasus[45], F. Polci[12], M. Poli Lener[22], M. Poliakova[67], A. Poluektov[10], N. Polukhina[80,c], I. Polyakov[67], E. Polycarpo[2], G. J. Pomery[53], S. Ponce[47], A. Popov[43], D. Popov[5,47], S. Popov[41], S. Poslavskii[43], K. Prasanth[33], L. Promberger[47], C. Prouve[45], V. Pugatch[51], A. Puig Navarro[49], H. Pullen[62], G. Punzi[28,n], W. Qian[5], J. Qin[5], R. Quagliani[12], B. Quintana[8], N. V. Raab[17], R. I. Rabadan Trejo[10], B. Rachwal[34], J. H. Rademacker[53], M. Rama[28], M. Ramos Pernas[55], M. S. Rangel[2], F. Ratnikov[41,81], G. Raven[32], M. Reboud[8], F. Redi[48], F. Reiss[12], C. Remon Alepuz[46], Z. Ren[3], V. Renaudin[62], R. Ribatti[28], S. Ricciardi[56], D. S. Richards[56], K. Rinnert[59], P. Robbe[11], A. Robert[12], G. Robertson[57], A. B. Rodrigues[48], E. Rodrigues[59], J. A. Rodriguez Lopez[73], A. Rollings[62], P. Roloff[47], V. Romanovskiy[43], M. Romero Lamas[45], A. Romero Vidal[45], J. D. Roth[84], M. Rotondo[22], M. S. Rudolph[67], T. Ruf[47], J. Ruiz Vidal[46], A. Ryzhikov[81], J. Ryzka[34], J. J. Saborido Silva[45], N. Sagidova[37], N. Sahoo[55], B. Saitta[26,f], D. Sanchez Gonzalo[44], C. Sanchez Gras[31], C. Sanchez Mayordomo[46], R. Santacesaria[30], C. Santamarina Rios[45], M. Santimaria[22], E. Santovetti[29,k], D. Saranin[80], G. Sarpis[61], M. Sarpis[74], A. Sarti[30], C. Satriano[30,q], A. Satta[29], M. Saur[5], D. Savrina[38,39], H. Sazak[9], L. G. Scantlebury Smead[62], S. Schael[13], M. Schellenberg[14], M. Schiller[58], H. Schindler[47], M. Schmelling[15], T. Schmelzer[14], B. Schmidt[47], O. Schneider[48], A. Schopper[47], M. Schubiger[31], S. Schulte[48], M. H. Schune[11], R. Schwemmer[47], B. Sciascia[22], A. Sciubba[30], S. Sellam[45], A. Semennikov[38], M. Senghi Soares[32], A. Sergi[47,52], N. Serra[49], J. Serrano[10], L. Sestini[27], A. Seuthe[14], P. Seyfert[47], D. M. Shangase[84], M. Shapkin[43], I. Shchemerov[80], L. Shchutska[48], T. Shears[59], L. Shekhtman[42,v], Z. Shen[4], V. Shevchenko[79], E. B. Shields[24,j], E. Shmanin[80], J. D. Shupperd[67], B. G. Siddi[20], R. Silva Coutinho[49], G. Simi[27], S. Simone[18,d], I. Skiba[20,g], N. Skidmore[74], T. Skwarnicki[67], M. W. Slater[52],

J. C. Smallwood[62], J. G. Smeaton[54], A. Smetkina[38], E. Smith[13], M. Smith[60], A. Snoch[31], M. Soares[19], L. Soares Lavra[9], M. D. Sokoloff[64], F. J. P. Soler[58], A. Solovev[37], I. Solovyev[37], F. L. Souza De Almeida[2], B. Souza De Paula[2], B. Spaan[14], E. Spadaro Norella[25,o], P. Spradlin[58], F. Stagni[47], M. Stahl[64], S. Stahl[47], P. Stefko[48], O. Steinkamp[49,80], S. Stemmle[16], O. Stenyakin[43], H. Stevens[14], S. Stone[67], M. E. Stramaglia[48], M. Straticiuc[36], D. Strekalina[80], S. Strokov[82], F. Suljik[62], J. Sun[26], L. Sun[72], Y. Sun[65], P. Svihra[61], P. N. Swallow[52], K. Swientek[34], A. Szabelski[35], T. Szumlak[34], M. Szymanski[47], S. Taneja[61], Z. Tang[3], T. Tekampe[14], F. Teubert[47], E. Thomas[47], K. A. Thomson[59], M. J. Tilley[60], V. Tisserand[9], S. T'Jampens[8], M. Tobin[6], S. Tolk[47], L. Tomassetti[20,g], D. Torres Machado[1], D. Y. Tou[12], M. Traill[58], M. T. Tran[48], E. Trifonova[80], C. Trippl[48], A. Tsaregorodtsev[10], G. Tuci[28,n], A. Tully[48], N. Tuning[31], A. Ukleja[35], D. J. Unverzagt[16], A. Usachov[31], A. Ustyuzhanin[41,81], U. Uwer[16], A. Vagner[82], V. Vagnoni[19], A. Valassi[47], G. Valenti[19], N. Valls Canudas[44], M. van Beuzekom[31], H. Van Hecke[66], E. van Herwijnen[80], C. B. Van Hulse[17], M. van Veghel[77], R. Vazquez Gomez[45], P. Vazquez Regueiro[45], C. Vázquez Sierra[31], S. Vecchi[20], J. J. Velthuis[53], M. Veltri[21,p], A. Venkateswaran[67], M. Veronesi[31], M. Vesterinen[55], D. Vieira[64], M. Vieites Diaz[48], H. Viemann[75], X. Vilasis-Cardona[83], E. Vilella Figueras[59], P. Vincent[12], G. Vitali[28], A. Vollhardt[49], D. Vom Bruch[12], A. Vorobyev[37], V. Vorobyev[42,v], N. Voropaev[37], R. Waldi[75], J. Walsh[28], C. Wang[16], J. Wang[3], J. Wang[72], J. Wang[4], J. Wang[6], M. Wang[3], R. Wang[53], Y. Wang[7], Z. Wang[49], D. R. Ward[54], H. M. Wark[59], N. K. Watson[52], S. G. Weber[12], D. Websdale[60], C. Weisser[63], B. D. C. Westhenry[53], D. J. White[61], M. Whitehead[53], D. Wiedner[14], G. Wilkinson[62], M. Wilkinson[67], I. Williams[54], M. Williams[63,68], M. R. J. Williams[57], F. F. Wilson[56], W. Wislicki[35], M. Witek[33], L. Witola[16], G. Wormser[11], S. A. Wotton[54], H. Wu[67], K. Wyllie[47], Z. Xiang[5], D. Xiao[7], Y. Xie[7], H. Xing[71], A. Xu[4], J. Xu[5], L. Xu[3], M. Xu[7], Q. Xu[5], Z. Xu[5], Z. Xu[4], D. Yang[3], Y. Yang[5], Z. Yang[3], Z. Yang[65], Y. Yao[67], L. E. Yeomans[59], H. Yin[7], J. Yu[70], X. Yuan[67], O. Yushchenko[43], K. A. Zarebski[52], M. Zavertyaev[15,c], M. Zdybal[33], O. Zenaiev[47], M. Zeng[3], D. Zhang[7], L. Zhang[3], S. Zhang[4], Y. Zhang[47], Y. Zhang[62], A. Zhelezov[16], Y. Zheng[5], X. Zhou[5], Y. Zhou[5], X. Zhu[3], V. Zhukov[13,39], J. B. Zonneveld[57], S. Zucchelli[19,e], D. Zuliani[27], G. Zunica[61]

[1] Centro Brasileiro de Pesquisas Físicas (CBPF), Rio de Janeiro, Brazil
[2] Universidade Federal do Rio de Janeiro (UFRJ), Rio de Janeiro, Brazil
[3] Center for High Energy Physics, Tsinghua University, Beijing, China
[4] School of Physics State Key Laboratory of Nuclear Physics and Technology, Peking University, Beijing, China
[5] University of Chinese Academy of Sciences, Beijing, China
[6] Institute of High Energy Physics (IHEP), Beijing, China
[7] Institute of Particle Physics, Central China Normal University, Wuhan, Hubei, China
[8] Univ. Grenoble Alpes, Univ. Savoie Mont Blanc, CNRS, IN2P3-LAPP, Annecy, France
[9] Université Clermont Auvergne, CNRS/IN2P3, LPC, Clermont-Ferrand, France
[10] Aix Marseille Univ, CNRS/IN2P3, CPPM, Marseille, France
[11] Université Paris-Saclay, CNRS/IN2P3, IJCLab, Orsay, France
[12] LPNHE, Sorbonne Université, Paris Diderot Sorbonne Paris Cité, CNRS/IN2P3, Paris, France
[13] I. Physikalisches Institut, RWTH Aachen University, Aachen, Germany
[14] Fakultät Physik, Technische Universität Dortmund, Dortmund, Germany
[15] Max-Planck-Institut für Kernphysik (MPIK), Heidelberg, Germany
[16] Physikalisches Institut, Ruprecht-Karls-Universität Heidelberg, Heidelberg, Germany
[17] School of Physics, University College Dublin, Dublin, Ireland
[18] INFN Sezione di Bari, Bari, Italy
[19] INFN Sezione di Bologna, Bologna, Italy
[20] INFN Sezione di Ferrara, Ferrara, Italy
[21] INFN Sezione di Firenze, Firenze, Italy
[22] INFN Laboratori Nazionali di Frascati, Frascati, Italy
[23] INFN Sezione di Genova, Genoa, Italy
[24] INFN Sezione di Milano-Bicocca, Milan, Italy
[25] INFN Sezione di Milano, Milan, Italy
[26] INFN Sezione di Cagliari, Monserrato, Italy
[27] Universita degli Studi di Padova, Universita e INFN, Padua, Italy
[28] INFN Sezione di Pisa, Pisa, Italy
[29] INFN Sezione di Roma Tor Vergata, Rome, Italy
[30] INFN Sezione di Roma La Sapienza, Rome, Italy
[31] Nikhef National Institute for Subatomic Physics, Amsterdam, The Netherlands

[32] Nikhef National Institute for Subatomic Physics and VU University Amsterdam, Amsterdam, The Netherlands
[33] Henryk Niewodniczanski Institute of Nuclear Physics Polish Academy of Sciences, Kraków, Poland
[34] Faculty of Physics and Applied Computer Science, AGH-University of Science and Technology, Kraków, Poland
[35] National Center for Nuclear Research (NCBJ), Warsaw, Poland
[36] Horia Hulubei National Institute of Physics and Nuclear Engineering, Bucharest-Magurele, Romania
[37] Petersburg Nuclear Physics Institute NRC Kurchatov Institute (PNPI NRC KI), Gatchina, Russia
[38] Institute of Theoretical and Experimental Physics NRC Kurchatov Institute (ITEP NRC KI), Moscow, Russia
[39] Institute of Nuclear Physics, Moscow State University (SINP MSU), Moscow, Russia
[40] Institute for Nuclear Research of the Russian Academy of Sciences (INR RAS), Moscow, Russia
[41] Yandex School of Data Analysis, Moscow, Russia
[42] Budker Institute of Nuclear Physics (SB RAS), Novosibirsk, Russia
[43] Institute for High Energy Physics NRC Kurchatov Institute (IHEP NRC KI), Protvino, Russia
[44] ICCUB, Universitat de Barcelona, Barcelona, Spain
[45] Instituto Galego de Física de Altas Enerxías (IGFAE), Universidade de Santiago de Compostela, Santiago de Compostela, Spain
[46] Instituto de Fisica Corpuscular, Centro Mixto Universidad de Valencia-CSIC, Valencia, Spain
[47] European Organization for Nuclear Research (CERN), Geneva, Switzerland
[48] Institute of Physics, Ecole Polytechnique Fédérale de Lausanne (EPFL), Lausanne, Switzerland
[49] Physik-Institut, Universität Zürich, Zurich, Switzerland
[50] NSC Kharkiv Institute of Physics and Technology (NSC KIPT), Kharkiv, Ukraine
[51] Institute for Nuclear Research of the National Academy of Sciences (KINR), Kyiv, Ukraine
[52] University of Birmingham, Birmingham, UK
[53] H.H. Wills Physics Laboratory, University of Bristol, Bristol, UK
[54] Cavendish Laboratory, University of Cambridge, Cambridge, UK
[55] Department of Physics, University of Warwick, Coventry, UK
[56] STFC Rutherford Appleton Laboratory, Didcot, UK
[57] School of Physics and Astronomy, University of Edinburgh, Edinburgh, UK
[58] School of Physics and Astronomy, University of Glasgow, Glasgow, UK
[59] Oliver Lodge Laboratory, University of Liverpool, Liverpool, UK
[60] Imperial College London, London, UK
[61] Department of Physics and Astronomy, University of Manchester, Manchester, UK
[62] Department of Physics, University of Oxford, Oxford, UK
[63] Massachusetts Institute of Technology, Cambridge, MA, USA
[64] University of Cincinnati, Cincinnati, OH, USA
[65] University of Maryland, College Park, MD, USA
[66] Los Alamos National Laboratory (LANL), Los Alamos, USA
[67] Syracuse University, Syracuse, NY, USA
[68] School of Physics and Astronomy, Monash University, Melbourne, Australia
[69] Pontifícia Universidade Católica do Rio de Janeiro (PUC-Rio), Rio de Janeiro, Brazil
[70] Physics and Micro Electronic College, Hunan University, Changsha, China
[71] Guangdong Provencial Key Laboratory of Nuclear Science, Institute of Quantum Matter, South China Normal University, Guangzhou, China
[72] School of Physics and Technology, Wuhan University, Wuhan, China
[73] Departamento de Fisica , Universidad Nacional de Colombia, Bogota, Colombia
[74] Universität Bonn-Helmholtz-Institut für Strahlen und Kernphysik, Bonn, Germany
[75] Institut für Physik, Universität Rostock, Rostock, Germany
[76] INFN Sezione di Perugia, Perugia, Italy
[77] Van Swinderen Institute, University of Groningen, Groningen, The Netherlands
[78] Universiteit Maastricht, Maastricht, The Netherlands
[79] National Research Centre Kurchatov Institute, Moscow, Russia
[80] National University of Science and Technology “MISIS”, Moscow, Russia
[81] National Research University Higher School of Economics, Moscow, Russia
[82] National Research Tomsk Polytechnic University, Tomsk, Russia

[83] DS4DS, La Salle, Universitat Ramon Llull, Barcelona, Spain
[84] University of Michigan, Ann Arbor, USA

[a] Universidade Federal do Triângulo Mineiro (UFTM), Uberaba, MG, Brazil
[b] Laboratoire Leprince-Ringuet, Palaiseau, France
[c] P.N. Lebedev Physical Institute, Russian Academy of Science (LPI RAS), Moscow, Russia
[d] Università di Bari, Bari, Italy
[e] Università di Bologna, Bologna, Italy
[f] Università di Cagliari, Cagliari, Italy
[g] Università di Ferrara, Ferrara, Italy
[h] Università di Firenze, Firenze, Italy
[i] Università di Genova, Genoa, Italy
[j] Università di Milano Bicocca, Milan, Italy
[k] Università di Roma Tor Vergata, Rome, Italy
[l] AGH - University of Science and Technology, Faculty of Computer Science, Electronics and Telecommunications, Kraków, Poland
[m] Università di Padova, Padua, Italy
[n] Università di Pisa, Pisa, Italy
[o] Università degli Studi di Milano, Milan, Italy
[p] Università di Urbino, Urbino, Italy
[q] Università della Basilicata, Potenza, Italy
[r] Scuola Normale Superiore, Pisa, Italy
[s] Università di Modena e Reggio Emilia, Modena, Italy
[t] Università di Siena, Siena, Italy
[u] MSU-Iligan Institute of Technology (MSU-IIT), Iligan, Philippines
[v] Novosibirsk State University, Novosibirsk, Russia